Highlights:

- C_{20} HBI δ^2H was measured in surface sediments of 12 lakes in the Adirondack Region
- δ^2H_{HBI} from lake diatoms reflects source water δ^2H
- HBI δ^2H and $\delta^{13}C$ vary with sampling water depth
- HBI δ^2H may be used as a lake water isotope proxy for paleohydrology applications

Hydrogen isotopic composition (δ^2H) of diatom-derived C_{20} highly branched isoprenoids from lake sediments track lake water δ^2H

Megan C. Corcoran[a*], Aaron F. Diefendorf[a], Thomas V. Lowell[a], Erika J. Freimuth[a], Anna K. Schartman[a], Benjamin R. Bates[a], Alexander K. Stewart[b], and Broxton W. Bird[c]

[a] Department of Geology, University of Cincinnati, Cincinnati, OH 45221-0013, USA

[b] Department of Geology, St. Lawrence University, Canton, NY 13617, USA

[c] Department of Earth Sciences, Indiana University-Purdue University, Indianapolis, IN 46202, USA

[*]Corresponding author.

E-mail address: megcorc@gmail.com (M. C. Corcoran)

Declaration of interests: none.

Highlights:

- C_{20} HBI δ^2H was measured in surface sediments of 12 lakes in the Adirondack Region
- δ^2H_{HBI} from lake diatoms reflects source water δ^2H
- HBI δ^2H and $\delta^{13}C$ vary with sampling water depth
- HBI δ^2H may be used as a lake water isotope proxy for paleohydrology applications

ABSTRACT

The hydrogen isotopic composition of lake water (δ^2H_{lw}) reflects hydrological processes, which can yield information about evaporation and precipitation changes through time when preserved in lake sediment archives. Unfortunately, few proxies exist that record only δ^2H_{lw}. Instead, most δ^2H_{lw} records represent a mix of aquatic and terrestrial material. Highly branched isoprenoids (HBIs), known to be produced by diatoms in marine and lacustrine settings, may be used as a lake water proxy to directly reconstruct hydroclimate if the hydrogen isotopic composition of HBIs (δ^2H_{HBI}) reflects the δ^2H_{lw}. We test this hypothesis by analyzing 78 sediment samples from 12 lakes in the Adirondack Mountains in New York for HBI concentrations and δ^2H. δ^2H_{HBI} was compared to δ^2H_{lw}, which showed an average fractionation ($\varepsilon_{HBI/lw}$) of -127.3 ± 15.0‰ (1σ) for all samples in all lakes. Consistency in $\varepsilon_{HBI/lw}$ between samples implies that δ^2H_{HBI} may be used to reconstruct δ^2H_{lw} through time to help assess how lake systems have changed in the past. Sediment samples collected from deeper (>4 m) zones within the lake had smaller variability in $\varepsilon_{HBI/lw}$ (±11.9‰, 1σ) than samples from shallower zones, suggesting that $\varepsilon_{HBI/lw}$ may be sensitive to other factors, such as light availability, which may be related to differences in diatom growth habit (e.g., benthic, planktonic). Similarly, the carbon isotopes of HBIs ($\delta^{13}C_{HBI}$) were higher for sediment samples collected in deeper zones in the lake, suggesting that $\delta^{13}C_{HBI}$ can be used to further differences in HBI synthesis in diatom communities living in different growth habitats.

Keywords: Hydrogen isotopes; highly branched isoprenoids; lake diatoms; aquatic biomarkers; paleohydrology; benthic; planktonic

1. Introduction

The hydrogen isotopic composition of lake water (δ^2H_{lw}) provides hydrologic information about source water δ^2H (e.g. precipitation) and the balance between evaporation and precipitation in lake systems (Gat, 1996; Henderson and Shuman, 2009; Anderson et al., 2016; Cluett and Thomas, 2020). Examining these processes in the past provides insights on the timing, magnitude, and controls on this essential cycle in order to improve future predictions of hydrological change. Materials preserved in lake sediment archives that capture δ^2H_{lw} can be used to generate records of these processes through time (Anderson et al., 2016). The δ^2H of various organic materials such as cellulose, and algal lipid biomarkers like sterols, botryococcenes, heptadecanes, phytadiene and fatty acids found in lake sediments, are utilized to track δ^2H_{lw} (Sauer et al., 2001; Zhang and Sachs, 2007). The δ^2H of plant waxes, also preserved in lake sediment archives, tracks plant source water δ^2H and is used to understand precipitation seasonality, precipitation amount, effective precipitation, and relative humidity through time (Sachse et al., 2012; Feakins et al., 2016; Thomas et al., 2016; Freimuth et al., 2017; Rach et al., 2017; Balascio et al., 2018; Thomas et al., 2020). Recent studies, however, illustrate that some lake sediment-derived plant wax compounds represent a mix of aquatic and terrestrial material (Hepp et al., 2015; Freimuth et al., 2020). For example, mid-chain plant wax δ^2H (C_{20}-C_{24} *n*-alkanes and alkanoic acids) is interpreted as a proxy for lake water δ^2H, but modern plant studies reveal that both aquatic and terrestrial plants can make these chain lengths (Tipple and Pagani, 2013; Thomas et al., 2016; Rach et al., 2017; Dion-Kirschner et al., 2020; Freimuth et al., 2020). C_{22} and C_{24} *n*-alkanoic acids are also identified as prominent constituents of suberin in root tissues (Graça and Santos, 2007; Pollard et al., 2008; Mueller et al., 2012; Holtvoeth et al., 2019). Reconstructing past lake water δ^2H would be simpler if the proxy were sourced from only species living in the lake. We tested the δ^2H of highly branched isoprenoids (HBIs), specifically the δ^2H of the C_{20} HBI compound (δ^2H_{HBI}) which are produced by lacustrine diatoms, and are abundant in many different lakes, (Rowland and Robson, 1990), to determine if δ^2H_{HBI} reflects δ^2H_{lw}.

Diatoms are single-celled eukaryotic microalgae found in aquatic settings that are used as bioindicators of a variety of environmental conditions such as pH, salinity, and other climate parameters (Charles, 1985; Charles et al., 1990; Dixit et al., 1992; Dixit et al., 1993; Smol and Stoermer, 2010; Rühland et al., 2015). For example, increases in the length of the ice-free season causes shifts in nutrient availability and light which were shown to increase diatom species diversity, specifically *Cyclotella* and *Asterionella* taxa in the Adirondack region of NY (Stager et al., 2017). Diatoms are found in a range of different lakes, except for hot and hypersaline lakes (Seckbach, 2019). Diatom growth habitats include benthic (bottom), planktonic (surface), and epiphytic (surface of plants) habitats (Patrick, 1977; Soininen and Teittinen, 2019) which can change as a function of environmental and climatological parameters (Laird et al., 2011; Rühland et al., 2015). The transitional depth from benthic to planktonic diatoms, or the benthic-planktonic depth in lacustrine settings, can be approximated using Secchi disk depth, an indicator of light availability, and has been used to assess past changes in drought (Laird et al., 2011). Modern relationships between diatom species assemblages and pH and salinity have been applied to sediment archives to reconstruct past lake chemistry and environmental parameters both spatially and temporally (Charles, 1985; Birks et al., 1990; Charles et al., 1990; Fritz et al., 1991; Dixit et al., 1993). For instance, on longer timescales, increasing salinity inferred from diatoms in the Northern Great Plains during the Early Holocene indicated a shift from a wet to a dry climate (Laird et al., 1998). Over the last 2 ka, in the northern prairies, analysis of diatom taxa indicated decadal to multidecadal shifts from wet to dry climates associated with changes in the North American jet stream (Laird et al., 2003); indicating that diatoms are sensitive to both local and synoptic-scale climate variability.

HBIs in sediments were first characterized in the Gulf of Mexico and later determined to be produced by diatoms in a variety of different environments (Gearing et al., 1976; Nichols et al., 1988; Rowland and Robson, 1990). HBIs vary in structure and by the length of carbon chains, with C_{20}, C_{25}, and C_{30} being the most commonly found compounds. C_{25} and C_{30} HBIs are more commonly found in marine environments, with overall concentrations of HBIs higher in oceanic settings than lake settings (Rowland and Robson, 1990; Sinninghe Damsté et al., 1999). One of the more common applications of HBIs has

been in marine settings with the use of IP_{25} as a proxy for sea ice (Nichols et al., 1988; Belt et al., 2001; Belt et al., 2007; Belt et al., 2017). In freshwater systems, C_{20} HBIs have been found in lakes, marshes and wetlands. C_{25} HBIs have been found in estuaries and lakes, while C_{30} is rarely found (Rowland and Robson, 1990; McKirdy et al., 2010; Pisani et al., 2013; He et al., 2015; He et al., 2016).

For C_{20} HBI, there is some speculation regarding the source of this compound and whether or not it is from diatoms and/or algal plants. The first report of C_{20} HBI in field samples associates this compound with algal plant samples (*Enteromorpha prolifera*) (Rowland et al., 1985). Follow up studies to this initial report indicated that the algal plants studied by Rowland et al. (1985) contained epiphytic diatoms, and therefore the exact source of the C_{20} HBIs is unclear (Rowland and Robson, 1990; Hird and Rowland, 1995). Some studies have reported C_{20} HBIs in lake sediments, including this study from the Adirondacks, from a range of lake water depths, suggesting that C_{20} HBIs are likely derived from planktonic, benthic, and possibly epiphytic diatom species, although other algal sources cannot be ruled out entirely without culture experiments.

Presently, few studies have examined HBIs from lacustrine diatoms and even fewer studies have explored the use of $\delta^{13}C$ and $\delta^{2}H$ of HBIs as a potential indicator of growth environment (Aichner et al., 2010; McKirdy et al., 2010; Balascio et al., 2011; Muschitiello et al., 2015). Balascio et al. (2011) used the concentrations of C_{20} and C_{25} HBIs to reconstruct changes in lake surface conditions throughout the Holocene in a coastal lake in Norway. Muschitiello et al. (2015) used the $\delta^{13}C$ of C_{20} HBIs as an indicator of tropic state in a lake in southern Sweden. McKirdy et al. (2010) used the $\delta^{13}C$ and $\delta^{2}H$ of C_{20} HBIs to examine a coastal wetland in South Australia over the past 7000 years to track lake ecology and local lake hydrology. Aichner et al. (2010) measured the $\delta^{2}H$ of C_{20} HBIs from the uppermost portion of a lake sediment core from the Tibetan Plateau and found similarities to the $\delta^{2}H$ of long-chain *n*-alkanes suggesting that $\delta^{2}H_{HBI}$, like plant wax $\delta^{2}H$, records source water $\delta^{2}H$ and is a promising tool that may be used to reconstruct past $\delta^{2}H_{lw}$ values.

The HBIs used in this study were discovered during analyses on plant waxes in Adirondack lakes (Fig. 1) (Freimuth et al., 2020; Schartman et al., 2020). Prior lake sediment work in the Adirondacks has investigated diatoms as means to understand lake chemistry and reconstruct past climate (Shero et al., 1978; Charles, 1984, 1985; Christie and Smol, 1986; Davis, 1987; Charles et al., 1990; Dixit et al., 1993; Stager et al., 2017). Charles (1985) characterized 240 diatom taxa from surface sediment of more than 30 lakes from the Adirondacks and found that the percent of planktonic diatom assemblages increased with lake water pH suggesting that diatoms can be used a proxy for past lake water chemistry in this region. Similarly, Dixit et al. (1993) found that over 20 diatom taxa from about 60 lakes in the Adirondacks may serve as an indicator of lake water pH with implications for understanding acidification processes in the Adirondacks watershed. Stager et al. (2017) linked increases in lake levels to increases in the relative amount of planktonic and tychoplanktonic (benthic or non-planktonic organisms that are transported into the water column by a disturbance) assemblages and used this to infer that there were greater precipitation amounts over the past 1600 years at Wolf Lake. Combined, these paleolimnological studies of diatoms from the Adirondacks provide evidence that diatom communities are recorders of environmental and climatological factors in this region.

Here, we test the hypothesis that δ^2H_{HBI} is a sensitive recorder of δ^2H_{lw}. We did this by measuring the δ^2H_{HBI} and δ^2H_{lw} from a suite of surface sediments from 12 lakes in the Adirondacks Park, NY, USA. We calculated the fractionation ($\varepsilon_{HBI/lw}$), or the quantitative link between δ^2H_{HBI} and δ^2H_{lw}, and discuss the potential applications of using δ^2H_{HBI} as a paleoclimate proxy. In addition, we explore the $\delta^{13}C$ of HBIs ($\delta^{13}C_{HBI}$) as a method of characterizing diatom growth habitat. δ^2H_{HBI} has the potential to provide δ^2H_{lw} and may provide a new way to reconstruct past hydrological processes in lake systems.

2. Methods:

2.1. Sample setting and collection

The Adirondack State Park, located in northern New York, is 24,000 km^2 and ranges from 37 to 1629 m above sea level with approximately 2,800 lakes covering over 1,000 km^2 of the park (Fig. 1) (Driscoll et al., 1991). The Adirondack Mountains are vegetated by both temperate broadleaf and mixed forest biomes (Olson et al., 2001). The modern Adirondacks climate is classified as humid-continental, with cold winters and cool summers (Peel et al., 2007). Modern climate datasets for the Adirondacks were obtained from the closest NOAA National Climatic Data Center station in Old Forge, NY (Fig. 1, 2) covering 1971–2010 (NOAA, 2020). Average monthly temperatures range from –9.9 °C to 17.9 °C between January and July (Fig. 2b) (NOAA, 2020). Average monthly precipitation amount is greatest during October with 127 mm and is lowest during February with 78 mm (Fig. 2c) (NOAA, 2020). Regional monthly precipitation isotopes were determined from the closest two sites with available data in the northeast, Ottawa, ON and Skaneateles, NY for 1972–2017 and 2015–2018 respectively. A seasonal cycle of precipitation δ^2H is observed with monthly averages between winter and summer ranging respectively from –110.5‰ to –40.1‰ in Skaneateles and –120.8‰ to –50.5‰ in Ottawa. (Fig. 2a) (Corcoran et al., 2019; IAEA/WMO, 2020).

Previous work on diatoms in Adirondack lakes examining diatoms has focused on watershed acidification where lake pH, alkalinity, conductivity and other lake water characteristics were measured in over 70 Adirondack lakes and compared to diatom assemblages (Charles, 1985; Dixit et al., 1993). Typical lake water pH and alkalinity in Adirondack lakes ranges from approximately 4.5 to 7.8 and from -31 to 408 μM respectively (Dixit et al., 1993). Conductivity in previously studied Adirondack lakes ranges from 11.9 to 58.7 $\mu S\ cm^{-1}$ (Dixit et al., 1993). Neither pH nor alkalinity were measured in this study; however, in eight of twelve lakes conductivity was measured which ranges from 8 to 79 $\mu S\ cm^{-1}$ (Table 1). Of all the Adirondacks lakes where diatoms were studied, Wolf Lake was the only one from this study that overlapped with previous diatom assemblage work (Table 1) (Stager et al., 2017). In Adirondack lakes, Secchi disk measurements, an indicator of the benthic-planktonic depth, ranged from

1.5 m to 9.6 m with a mean depth of 5.5 (Charles et al., 1990). More specifically, in Wolf Lake, Secchi disk measurements have ranged from 3 m to 5 m since 2012 (Stager et al., 2017). In Chazy Lake and Raquette Lake, average Secchi disk measurements were 4.1 m and 3.7 m, respectively (Laxson et al., 2019). Secchi disk depth was not measured in the 12 study lakes.

Surface sediment samples (n = 78) were collected from 12 lakes in the Adirondacks State Park, NY in October 2016 and January 2017 (Fig. 1). Details of the sampling sites and lake size are reported in Table 1. About half of the samples (n = 42) were taken using a square rod piston corer and polycarbonate tubing. Sub-sampling for these sediment cores was conducted at 1, 5 and 9 cm depths. The remaining samples (n = 36) were taken using a gravity corer which collected sediment cores of about 30 cm in length. The top 5 cm of each of these cores were homogenized and used for analysis. The sediment water interface was intact during core recovery for both methods used. Specific sampling depths and technologies are reported in Appendix A. Supplementary Material Table S1. Based on ^{210}Pb dating of sediment from 10 cm depths from Heart Lake, Moose Pond, Wolf Lake, Debar Lake and East Pine Pond, the age at that depth of the sediment core ranged from calendar year 1960 to 2004 (Freimuth et al., 2020). Based on this and ^{210}Pb dating of other Adirondack lakes the sediments samples from this study represent the last 50 years indicating that measurements taken in this study are an average of the last 50 years (Binford, 1990; Binford et al., 1993).

A total of 96 water samples from lakes throughout the Adirondacks were collected in October 2016, January 2017, May 2017, June 2019, and July 2019. Mean annual lake water isotopic composition was calculated for each of the 12 lakes sampled for HBIs in this study. In addition, seven precipitation samples and three ground snow samples were collected during sediment sampling campaigns in the Adirondacks. The collective analysis reported here expands that of water isotope data that was previously published, along with additional sampling information, site descriptions, and sediment chronologies (Freimuth et al., 2020; Schartman et al., 2020).

2.2. Extraction and fractionation

The lipid extraction and separation techniques used for this study were previous described by Freimuth et al. (2020). In summary, sediment samples were freeze dried and homogenized. Samples were extracted by accelerated solvent extraction (ASE; Dionex 350) with 9:1 (v/v) dichloromethane/methanol (DCM/MeOH) using three extraction cycles at 100 ºC and 10.3 MPa. The total lipid extract was then saponified with 3 ml of 0.5 N potassium hydroxide (KOH) in MeOH/H_2O (3:1, v/v) for 2 h at 75 ºC, then 2.5 mL of NaCl in water (5%, w/w) was added and acidified with 6N HCl to a pH < 2. The solution was extracted with hexanes/DCM (4:1, v/v), the resultant extract was neutralized with $NaHCO_3$/H_2O (5%, w/w), and water removed by addition of anhydrous Na_2SO_4. Neutral and acid fractions were separated using DCM/IPA (2:1, v/v) and 4% formic acid in diethyl ether, respectively, over aminopropyl-bonded silica gel. The neutral fraction was then separated into aliphatic and polar fractions using activated alumina oxide column chromatography. The aliphatic fraction was separated over 5% silver nitrate impregnated silica gel with hexanes to collect saturated compounds. This fraction was analyzed for HBIs and their concentrations.

Prior to isotope analysis, the saturated aliphatic fraction was further purified to separate *n*-C_{17} alkane from the C_{20} HBI with urea adduction (see section 2.4 for details on why this method was needed for these samples (Fig. 3a, b). The C_{20} HBI was separated by adducting the *n*-alkanes in urea crystals with equal parts 10% urea in methanol (w/w), acetone, and *n*-pentane by freezing at –20ºC for >1 hr and subsequent evaporation with nitrogen. Non adducts, containing the HBIs, were extracted by rinsing the urea crystals with hexanes.

2.3. HBI assignment and quantification

HBIs were identified on an Agilent 7890A gas chromatograph (GC) and Agilent 5975C quadrupole mass selective detector (MSD), operated at 70 eV, and quantified using a flame ionization detector (FID) (Fig. 3c). A multimode inlet was used and operated in pulsed spitless mode at a constant temperature of 320 ºC.

Compounds were separated on a fused silica column (Agilent J&W DB-5ms; 30 m x 0.25 mm, 25 μm film) fitted with a guard column (Restek Rxi, 5 m, 0.32 mm ID), with a helium flow of 1 mL min^{-1}, and the oven ramped from an initial temperature of 60 ºC (held 1 min) to 320 ºC (held 15 min) at 6 ºC min^{-1}. Following GC separation, the column effluent was split (1:1) between the FID and MSD with a 2-way splitter with He makeup to keep pressure constant. HBIs were identified using published spectra (Rowland et al., 1985; Rowland and Robson, 1990; Volkman et al., 1998; Belt et al., 2000; Balascio et al., 2011). Additionally, samples were ion extracted for characteristic HBI ions to determine if there were additional HBIs. Only the C_{20} HBI was detected in these lake sediments.

For quantification, samples were diluted in hexanes spiked with 1,1'-binaphthyl as an internal standard prior to quantification. Compound peak areas were normalized to those of 1,1'-binaphthyl and converted to concentration using response curves for an in-house mix of *n*-alkanes (even-chains from C_{14} to C_{18}; odd-chains from C_{25} to C_{35}) and FAMEs (C_{16}, C_{18}, C_{24}, C_{28}, C_{30}) at concentrations ranging from 0.5 to 100 μg mL^{-1}. Precision and accuracy were determined by analyzing external standards at 25 μg mL^{-1} as unknowns and were 0.61 (1σ, n = 13) and 0.41 (1σ, n = 13), respectively (HBIs were quantified along with alkane concentrations reported in Freimuth et al. (2020)). Quantified concentrations were normalized to the mass of dry sediment. Recovery standards were not used because extractions were initially focused on isotopes of plant waxes, however, for other lake sediment projects in our lab, this is typically > 90% (before urea adduction).

2.4. HBI isotopic analysis

The δ^2H of the C_{20} HBI was determined using a Thermo Trace GC Ultra coupled to an Isolink pyrolysis reactor (1420 ºC) and interfaced to a Thermo Electron Delta V Advantage IRMS via a Conflo IV. Samples were dissolved in hexanes and injected (1 to 5 μL) into a programmed temperature vaporization inlet at 60 ºC (held 1 min; He flow of 1.4 mL min^{-1}), heated to 300 ºC at 14.5 ºC s^{-1} and held for a transfer time of 1 min, and then heated to 350 ºC for a cleaning phase of 6 min (with He flow of 120 mL min^{-1}).

The GC column was the same as above. The GC oven program started at 60 ºC (held 2 min), ramped to 150 ºC (15 ºC min^{-1}), then to 180ºC (4 ºC min^{-1}), and then to 320 ºC (20 ºC min^{-1}; held 15 min). We also found that our standard *n*-alkane GC oven program with an initial temperature of 80 ºC (held 2 min), heated to 170 ºC (15 ºC min^{-1}), and then heated to 320 ºC (held 15 min) was also suitable, but the previous method has higher throughput and therefore we used that for data reported here. Neither method could separate the C_{20} HBI from *n*-C_{17} alkane with sufficient baseline separation for isotopic analysis, even when *n*-C_{17} alkane was at low abundance (Fig 3b). During preliminary method testing, we found that the δ^2H of the *n*-C_{17} alkanes were often 100 to 200‰ different from the δ^2H of the HBIs and therefore had a strong effect on the δ^2H of the C_{20} HBI, either due to a memory effect or due to the background correction. Therefore, all samples were further purified with urea adduction prior to isotope analysis. The H_3^+ factor was tested daily and averaged 4.5 ppm nA^{-1} during the period of analysis. The isotopic composition of samples was normalized to the VSMOW/VSLAP scale using periodic interspersed standards of known δ^2H composition (Mix A6, A. Schimmelmann, Indiana University) and are reported in standard delta notation. Additionally, an in-house standard was also analyzed every ~8 samples (Oak-1a). We determined the analytical precision to be 4.6‰ by pooling the standard deviation from all replicates following Polissar and D'Andrea (2014). The precision on the Oak-1a standard is 1.8 and 2.0‰ δ^2H (1σ, n = 42) for *n*-C_{29} and *n*-C_{31} alkane, respectively. The accuracy on the Oak-1a standard is 0.01 and 0.7‰ (n = 42) for *n*-C_{29} and *n*-C_{31} alkane, respectively, and was determined from prior Oak-1a analyses (n = 76).

For $\delta^{13}C$, the same GC-IRMS was used but was fitted with a combustion reactor packed with Pt, Cu, and Ni wires at 1000°C. The reactor was oxidized for 1 min prior to each run and for 1 hr every ~50 injections (or when $\delta^{18}O$ deviated more than 0.5‰). The isotopic composition of samples was normalized to the VPDB scale using periodic interspersed standards of known $\delta^{13}C$ composition (Mix A6, A. Schimmelmann, Indiana University) and are reported in standard delta notation. Additionally, an in-house standard was also analyzed every ~8 samples (Oak-1a). The pooled analytical precision was 0.2‰ (Polissar and D'Andrea, 2014). Additionally, C_{14} and C_{15} *n*-alkanes were co-injected with all samples and

standards and their precision and accuracy, for sample runs, were 0.2‰ (1σ, n = 35) and –0.08‰ (n = 35) for C_{14} and 0.2‰ (1σ, n = 35) and –0.04‰ for C_{15}, respectively.

2.5. Lake water δ^2H analysis

Samples collected before June 2019 were analyzed on a Picarro L2130-*i* cavity ring-down spectrometer water isotope analyzer at Indiana University-Purdue University (van Geldern and Barth, 2012). Samples collected in June and July 2019 were analyzed on a GasBench-IRMS at the University of Cincinnati by headspace analysis and equilibration with H_2 and CO_2 gases at 25 ºC. Samples were normalized to the VSMOW/SLAP scale using lab standards calibrated with SMOW2, SLAP2, and GISP. Instrument precision was 0.06‰ for $\delta^{18}O$ and 0.2 for δ^2H at Indiana University-Purdue University and 2.0‰ for $\delta^{18}O$ and 2.6‰ for δ^2H at University of Cincinnati.

2.6. Biosynthetic fractionation between HBI δ^2H and lake water δ^2H:

Hydrogen fractionation (ε_{bio} or $\varepsilon_{HBI/lw}$) for each sample between δ^2H_{HBI} and δ^2H_{lw} was calculated using the following equation:

$$\varepsilon_{(HBI/lw)} = \left(\frac{(\delta^2H_{HBI} + 1000)}{(\delta^2H_{lw} + 1000)} - 1\right)$$

Fractionation values were calculated using mean annual δ^2H_{lw} in addition to seasonal δ^2H_{lw} from samples collected in January, May, June, July and October (Table S2).

3. Results:

3.1. Observed diatom HBIs

The C_{20} HBI diatom biomarker was present in 61 surface sediment sediments from 11 of the 12 total lakes in the Adirondacks region. In all samples studied here, C_{20} HBI was found whereas the diatom-derived C_{25} and C_{30} HBIs were absent. HBIs described in the remainder of this text refer only to the C_{20} HBI. Concentrations of HBIs in all lake sediments ranges from 0.9 to 81.9 μg g^{-1} dry sediment with an average concentration of 15.3 ± 17 μg g^{-1} dry sediment (1σ), (Table S1). There is no observed relationship between HBI concentration and water depth. HBI concentrations are highest in Raquette Lake, Sucker Lake and Wolf Lake with average HBI concentrations of 53.4 ± 3 μg g^{-1} dry sediment (1σ), 54.8 ± 30 μg g^{-1} dry sediment (1σ) and 52.0 ± 8 μg g^{-1} dry sediment respectively. Horseshoe Lake has the lowest HBI concentration, averaging 3.0 ± 1 μg g^{-1} dry sediment (1σ).

3.2. Hydrogen isotopes of lake water

The range of δ^2H_{lw} from all lake water samples collected in the Adirondacks is –83.2‰ to –41.8‰ (Fig. 4a). The highest δ^2H_{lw} is observed in October 2016 where δ^2H_{lw} ranges from –65‰ and –41.8‰ (Fig. 4b). The lowest δ^2H_{lw} is observed in June and ranges between –83.2‰ and –62.1‰ (Fig. 4b), however seasonal variation is minimal in δ^2H_{lw} when compared to precipitation δ^2H. Mean annual δ^2H_{lw} for all ten sampled lakes that were measured for δ^2H_{HBI} ranges from –74.1‰ to –53.1‰. Precipitation δ^2H from samples (n = 7) collected during sediment sampling campaigns ranged from –101.9‰ and –37.0‰ between November and July (Fig 4a). Ground snow δ^2H collected in October (n = 2) and January (n=1) are –81.6‰, –115.7‰ and –118.2‰ respectively (Fig. 4a).

3.3. Hydrogen isotopes of C_{20} HBIs

Of the 61 surface sediments measured here, 42 samples had HBIs of high enough concentrations to measure δ^2H. Measured δ^2H_{HBI} ranges from –209.4‰ to –160.4‰ with a mean of –183.2 ± 12.6‰ (1σ).

Calculated $\varepsilon_{HBI/lw}$ values for all samples between δ^2H_{HBI} and δ^2H_{lw} ranges from –165.0‰ to –104.4‰ (Fig. 5a) with a mean of –127.3 ± 15.0‰ (1σ). Lower (more negative) $\varepsilon_{HBI/lw}$ values correspond to shallow water depths of sampling with a slight relationship between $\varepsilon_{HBI/lw}$ and water depth (least squares linear regression; $R^2 = 0.22$, $p = 0.002$) (Fig. 5a). In order to explore this relationship further, samples were divided into two subgroups, samples taken above and below 4 m of water depth. This depth was determined from the best estimate of the benthic-planktonic depth based on previous Secchi disk depth measurements from three of the Adirondack lakes from this study (See Section 2.1). Samples collected when water depth was <4 m have a mean $\varepsilon_{HBI/lw}$ of –143.7 ± 19.0‰ (1σ, n = 10), whereas samples collected at water depths >4 m have a mean of –123.0 ± 11.9‰ (1σ, n = 32) (Fig. 5). These sample subsets are significantly different from one another (*t*-test, p = 0.017; Fig. 5b). We acknowledge that this 4 m depth is arbitrary given that Secchi disk depth was not measured in every lake. To explore this further, we divided the data into subgroups above and below depths of 3 m or 5 m, the maximum and minimum Secchi disk depths reported for some of these lakes. The separation at 3 m depth was significant (*t*-test, p = 0.0002), but not at 5 m depth was not significant (p = 0.15). East Pine Pond is the only lake where we sampled above and below 4 m depth in the same lake and $\varepsilon_{HBI/lw}$ values in this lake fit the overall pattern of more negative values in the shallow zone. Future work will need to explore the importance of light availability and compare benthic and pelagic diatom assemblages that produce C_{20} HBIs. Regardless, deeper samples have lower variability (± 11.9‰).

To explore if changes in δ^2H_{lw} influence δ^2H_{HBI}, we calculated $\varepsilon_{HBI/lw}$ using mean δ^2H_{lw} in addition to January, May, July and October δ^2H_{lw}. Mean $\varepsilon_{HBI/lw}$ for all samples calculated using January, May, July and October δ^2H_{lw} are –124.0 ± 12.1‰, –120.1 ± 13.6‰, –129.3 ± 15.7‰ and –132.6 ± 15.9‰, respectively (Table S2). Because δ^2H_{lw} only changes about 12‰ throughout the year, it appears that $\varepsilon_{HBI/lw}$ does not vary seasonally in these Adirondack lakes (see Section 4.1). To eliminate sampling bias caused by the different numbers of samples collected at each of the lakes, we calculated a lake $\varepsilon_{HBI/lw}$

mean. Comparisons between the mean of the lake $\varepsilon_{HBI/lw}$ means (–126.6‰) and the mean of all $\varepsilon_{HBI/lw}$ samples (–127.3‰) are similar suggesting that no one lake is biasing the sample mean $\varepsilon_{HBI/lw}$.

3.4. Carbon isotopes of C_{20} HBIs

A total of 38 samples were measured for $\delta^{13}C_{HBI.}$ The measured $\delta^{13}C_{HBI}$ for all lakes ranges from –32.2‰ to –21.5‰ with a mean of –27.1 ± 2.2‰ (1σ) (Fig. 5c). Samples collected at water depths >4 m and <4 m (see above section) have a mean –26.6 ± 1.9‰ (1σ, n = 29) and –29.7 ± 1.9‰ (1σ, n = 9), respectively (Fig. 5). $\delta^{13}C_{HBI}$ of samples taken at depths >4 m is statistically different to samples taken at depths <4 m (*t*-test, $p = 0.0004$) (Fig. 5d). In East Pine Pond, the $\delta^{13}C_{HBI}$ of the sample taken at 1.8 m water depth is –30.4‰ whereas the $\delta^{13}C_{HBI}$ of the sample taken at 10 m water depth is –25.8‰ (Fig. 5c). East Pine Pond has the greatest range in $\delta^{13}C_{HBI}$, –30.4‰ to –24.6‰. The most ^{13}C-enriched $\delta^{13}C_{HBI}$ sample is from Little Green Pond (–21.5‰) and the most ^{13}C-depleted $\delta^{13}C_{HBI}$ samples are from Quiver Lake (–32.1‰) and Raquette Lake (–31.9‰). Unfortunately, $\delta^{13}C$ of the dissolved inorganic carbon was not measured. Therefore, we can only speculate below as to why $\delta^{13}C_{HBI}$ varies with depth and among lakes.

4. Discussion:

4.1. C_{20} HBI δ^2H as an indicator of lake water δ^2H

Hydrogen isotopes of lake water (δ^2H_{lw}) are widely used to reconstruct hydrological processes such as precipitation (Gat, 1996; Henderson and Shuman, 2009; Anderson et al., 2016). The hydrogen isotopic fractionation between source water and lipid biomarker is required in order to accurately reconstruct these processes from biomarker lipids. Consistency of fractionation values indicate that proxy δ^2H reflects source water δ^2H and can be applied to sediment archives to reconstruct past hydroclimate (Sachse et al.,

2012) . Overall, we observe similar fractionation values ($\varepsilon_{HBI/lw}$) between δ^2H_{HBI} and deep δ^2H_{lw} for ten lakes in the Adirondacks suggesting that δ^2H_{lw} can be inferred using δ^2H_{HBI} (Fig. 5a). The variation observed in $\varepsilon_{HBI/lw}$ may be due to biological or climatological effects such as the seasonality of HBI production and differences in sampling water depth (see below). We observe an uncertainty of about ± 12‰ in $\varepsilon_{HBI/lw}$ between deep samples in this study. The range observed here is similar to the range of apparent fractionation of other δ^2H molecular proxies such as plant wax *n*-C_{28} alkanoic acid δ^2H and *n*-C_{29} alkane δ^2H in sediments, whose fractionation is –99 ± 32‰ and –121 ± 18‰ respectively (McFarlin et al., 2019).

In comparison to another C_{20} δ^2H_{HBI} study, core top sediment from a lake on the Tibetan Plateau has a fractionation value of –90.2‰ between measured C_{20} δ^2H_{HBI} and precipitation δ^2H from that region, as δ^2H_{lw} was not reported (Aichner et al., 2010). This fractionation value falls close to the range of the Adirondack samples and would likely be lower (more negative) if δ^2H_{lw} had been used because of the arid climate in the region (Aichner et al., 2010). Evaporative enrichment of lake water due to high aridity in this region causes greater evaporation of lake water resulting in ^2H-enriched lake water and ultimately more negative $\varepsilon_{HBI/lw}$.

Our results suggest that δ^2H_{HBI} is a sensitive recorder of δ^2H_{lw}. However, the variations in $\varepsilon_{HBI/lw}$ within and between lakes could suggest that other factors may influence $\varepsilon_{HBI/lw}$. The timing of diatom HBI biosynthesis is unlikely to influence $\varepsilon_{HBI/lw}$ in these Adirondack lakes because changes in δ^2H_{lw} are minimal throughout the year (Fig. 4b). If δ^2H_{lw} changes seasonally, then $\varepsilon_{HBI/lw}$ would be biased towards the time of the year that HBIs are biosynthesized. Regional observations and modelled precipitation δ^2H show that precipitation δ^2H varies seasonally between −235.9‰ to +24.2‰ from winter to summer (Fig. 4a) (Bowen and Revenaugh, 2003; Corcoran et al., 2019; Bowen, 2020; IAEA/WMO, 2020). δ^2H_{lw}, however, only varies slightly throughout the year relative to the distinct seasonal variations observed in precipitation δ^2H (Fig. 4b), due to long lake water residence times, or the time it takes to completely flush

the lake. δ^2H_{lw} values are also similar to mean annual precipitation δ^2H in the Adirondack lakes, largely because these lakes have low evaporation rates (Fig. 4). Because there is only a slight seasonal change in δ^2H_{lw}, the timing of diatom HBI biosynthesis appears unlikely to influence $\varepsilon_{HBI/lw}$ in these lakes. This is further supported by the small variation of $\varepsilon_{HBI/lw}$ when calculated by using δ^2H_{lw} from different seasons (see section 3.3, Table S2). However, this may not be the case in lakes from other regions where δ^2H_{lw} varies substantially through the year, such as open lakes with very short water residence times (e.g., Henderson and Schuman, 2009; Cluett and Thomas, 2020). Thus, in this suite of lakes from the Adirondacks, it is unlikely that variations in $\varepsilon_{HBI/lw}$ are due to differences in the seasonality of HBI production or δ^2H_{lw} changes and may be due to biological effects instead.

Lake water stratification is also unlikely to influence δ^2H_{lw} and thus $\varepsilon_{HBI/lw}$ in these lakes. Adirondack lakes are dimictic with little seasonal variation in δ^2H_{lw} (see above) suggesting that stratification of lake water causes little or no variation in δ^2H_{lw}. This indicates that changes in the source water of the HBIs, δ^2H_{lw}, is an unlikely a cause of both the general differences and difference observed by depth in $\varepsilon_{HBI/lw}$.

We hypothesize that differences in diatom growth habitats, benthic versus planktonic, may explain some of the variations in $\varepsilon_{HBI/lw}$ with water depth. This study was not designed to test epiphytic diatoms, so we cannot rule out their contribution to benthic samples and how they may influence $\varepsilon_{HBI/lw}$. Because there is variation in $\varepsilon_{HBI/lw}$ above and below benthic-planktonic depth boundary, best estimated to be about 4 m in these studies lakes, this may be a major biological factor influencing fractionation. In shallow waters above this transition, light penetrates lake water to the sediment allowing for both benthic and planktonic diatoms. Below this transition, light cannot penetrate to the sediments and therefore diatoms are planktonic. Some benthic diatoms, however, might be reworked from shallower sediments to deeper sediments through littoral processes. Many of the samples studied here were collected well below the benthic-planktonic depth boundary and therefore the majority of HBIs captured in these sediments are most likely derived from planktonic diatoms. This suggests that the differences in $\varepsilon_{HBI/lw}$ between shallow

(more negative $\varepsilon_{HBI/lw}$) and deep zones are due to this difference in growth habitat. Future work will have to confirm these findings.

If these differences in $\varepsilon_{HBI/lw}$ were related to growth habit, then there may be differences in the biosynthesis of the C_{20} HBI between benthic and planktonic diatom species. Diatoms synthesize HBIs from isopentenyl diphosphate (IPP), the main building block of all terpenoids. In diatoms, IPP is synthesized within the mevalonate (MVA) and methylerythritol phosphate (MEP) pathways in the cytosol and the plastid, respectively, and is very similar to terpenoid synthesis in higher plants (Massé et al., 2004; Diefendorf et al., 2012). IPP can also be shared between the cytosol and plastid. Of the few diatom species studied, C_{25} and C_{30} HBIs have been shown to be synthesized from either pathway, despite HBIs being found in the cytosol, with a marine planktonic species producing HBIs in the MVA pathway and a marine benthic species producing HBI in the MEP pathway (Massé et al., 2004; Athanasakoglou et al., 2019). Due to differences in the biosynthetic steps between these two pathways (NADPH requirements), the δ^2H of IPP and thus HBI, are likely to be different. Very little is known, unfortunately, about which species make these HBIs and how they are synthesized, especially for the C_{20} HBI. Because of the similarity in $\varepsilon_{HBI/lw}$ in the >4 m samples, we speculate that these planktonic diatoms are using one pathway to synthesize the HBIs. However, in the shallow samples, the mix of benthic and planktonic species, possibly utilizing both pathways, may cause the wider variation in $\varepsilon_{HBI/lw}$. This mixing of species habits may be important to consider if examining HBIs from both planktonic and benthic communities for paleo applications (see below).

4.2. HBI $\delta^{13}C$ as an indicator of diatom growth habitat

We explored the relationship between $\delta^{13}C_{HBI}$ and lake water depth to determine if it could be used as an indicator of diatom growth habitats, especially for paleo down-core applications. Overall, the $\delta^{13}C_{HBI}$ values were lower in samples collected at shallow water depths (<4 m) compared to the deeper samples

(Fig. 5c, d). This $\delta^{13}C_{HBI}$ relationship with depth may be related to changes in the $\delta^{13}C$ of dissolved inorganic carbon ($\delta^{13}C_{DIC}$) that often varies in the water column by depth and by productivity. In lake systems, $\delta^{13}C_{DIC}$ is a function of mixing between atmospheric $\delta^{13}C$ ($\delta^{13}C_{atm}$), sediment respired CO_2 ($\delta^{13}C_{resp}$), and productivity (Bade et al., 2004; Leng and Marshall, 2004). $\delta^{13}C_{resp}$ is ^{13}C-depleted compared to $\delta^{13}C_{atm}$ resulting in the $\delta^{13}C_{DIC}$ in lake systems to be more ^{13}C-enriched at the lake water surface than at the sediments at the bottom of the lake (Miyajima et al., 1997; Bade et al., 2004; Leng and Marshall, 2004; Diefendorf et al., 2008). Benthic diatom communities are likely using respired CO_2 from the decomposition of organic matter as a carbon source causing the $\delta^{13}C_{HBI}$ to be ^{13}C-depleted (He et al., 2016). In addition to the differences in the uptake of respired carbon, the lake productivity will influence $\delta^{13}C_{HBI}$ (Hollander and McKenzie, 1991; Bade et al., 2004). Productivity influences $\delta^{13}C_{DIC}$ values in the upper water column, where productivity is high, through the removal of ^{13}C-depleted organic matter resulting in ^{13}C-enriched $\delta^{13}C$ values (Herczeg, 1987; Hollander and McKenzie, 1991). HBIs of planktonic diatom communities that are preserved in deep water sediments will therefore have ^{13}C-enriched $\delta^{13}C$ values relative to the benthic diatom community $\delta^{13}C$ values because of high productivity in the upper water column. This contrasts with diatoms living in the shallow parts of the lake where both benthic and planktonic communities are incorporated, resulting in HBIs preserved in these sediments to show a more respired carbon signal, less of a productivity signal, and therefore ^{13}C-depleted $\delta^{13}C$ values. The $\delta^{13}C_{HBI}$ values of samples taken at depths >4 m were significantly higher than the $\delta^{13}C_{HBI}$ values of samples taken at depths <4 m (see section 3.4). This suggests that $\delta^{13}C_{HBI}$ values may be used to determine the growth habitat of the diatoms synthesizing HBIs. This may be useful for constraining $\varepsilon_{HBI/lw}$ for paleo reconstructions of $\delta^{2}H_{lw}$.

4.3. C_{20} HBI as a lake water $\delta^{2}H$ proxy and paleoclimate implications

This modern calibration dataset illustrates the potential for reconstructing past δ^2H_{lw} using HBIs extracted from sediment archives. Depending on the lake system of interest, records of δ^2H_{lw} derived from δ^2H_{HBI} can be used to generate past records of lake water evaporation (hydrologically closed systems) or precipitation (hydrologically open systems (Cluett and Thomas, 2020). For example, in hydrologically closed evaporative lakes, δ^2H_{HBI} may be combined with other proxies that record precipitation δ^2H, such as the δ^2H of terrestrial plant waxes, (Sachse et al., 2012; Freimuth et al., 2020) to quantify the extent of evaporation (Henderson and Shuman, 2009; Anderson et al., 2016; Rach et al., 2017).

Unlike other lake water isotopic proxies, δ^2H_{HBI} can be used to create records of past δ^2H_{lw} without complications of mixed source material. Although there are terrestrial diatoms that are found in soils, C_{20} HBI producing diatoms have only been documented in aquatic species (Rowland and Robson, 1990; McKirdy et al., 2010; He et al., 2016). Mid-chain length alkanoic acids and *n*-alkanes from plant waxes are often shown to be produced by aquatic plants and have been used to reconstruct δ^2H_{lw} (Thomas et al., 2016; Rach et al., 2017; Thomas et al., 2020). However, modern calibration studies of plant waxes from land plants illustrate that mid-chain length alkanoic acids and *n*-alkanes can be derived from both terrestrial and aquatic plants (Freimuth et al., 2017; Berke et al., 2019; Dion-Kirschner et al., 2020), and whether or not they can be used to track lake water may largely depend on the location and the types of terrestrial and aquatic plants present (Chikaraishi and Naraoka, 2003; Sachse et al., 2012; Thomas et al., 2016; Berke et al., 2019; McFarlin et al., 2019). In addition, mid-chained C_{22} and C_{24} fatty acids have been identified as one of the major components of suberin in root tissue (Graça and Santos, 2007; Pollard et al., 2008; Holtvoeth et al., 2019). This indicates that records of these compounds may be from mixed source material and the δ^2H may reflect some combination of δ^2H_{lw} and δ^2H of the plant root water or soil water. Similarly, oxygen isotopes ($\delta^{18}O$) of cellulose and hemi-cellulose extracted from lake sediment have been used to reconstruct lake water $\delta^{18}O$ to reconstruct paleohydrology, but assumptions about sources are an issue as materials can be both terrestrial and aquatic (Wolfe et al., 2007; Hepp et al., 2015; Street-Perrott et al., 2018; Jones et al., 2019). Records of δ^2H_{lw} from δ^2H_{HBI} could reduce complexities in

hydroclimate interpretations by eliminating uncertainties associated with mixing of aquatic and terrestrial sourcing through time.

Diatoms are spatially diverse in lacustrine settings suggesting that HBI compounds can be found in a variety of environments at different latitudes (Soininen and Teittinen, 2019). δ^2H_{HBI} will be useful for paleoclimate reconstructions in a wide array of ecosystems as opposed to other spatially limited lake water isotope proxies (e.g. carbonate $\delta^{18}O$).

In order to avoid complexities with capturing both planktonic and benthic communities in paleo-applications, sampling lake depocenters that are far below the depth of light penetration will help to restrict the HBIs to planktonic communities. If this is the case, reconstructions of δ^2H_{lw} from δ^2H_{HBI} will utilize the $\varepsilon_{HBI/lw}$ from the deep samples ($-123.0 \pm 11.9‰$, 1σ) instead of the $\varepsilon_{HBI/lw}$ of all samples. Additionally, records of $\delta^{13}C_{HBI}$ from sediment cores may be used to screen for past changes in diatom growth habits. For example, shifts to more ^{13}C-enriched $\delta^{13}C_{HBI}$ should suggest a shift to more planktonic diatom communities or a shift in the benthic-planktonic depth boundary. Constraining growth habitats through time using $\delta^{13}C_{HBI}$ and sampling in deep lake locations will aid in climate interpretations of δ^2H_{HBI}.

4.4. Future directions

This preliminary dataset indicates that using δ^2H_{HBI} as an aquatically sourced molecular proxy for source water δ^2H (δ^2H_{lw}) has the potential to answer hydrological questions of how lake systems change through time. Additional measurements of δ^2H_{HBI} and δ^2H_{lw} from a diversity of ecosystems will expand this dataset of $\varepsilon_{HBI/lw}$ and help identify other environmental factors that may influence δ^2H_{HBI} beyond source water δ^2H. As discussed in Section 4.1, growth habit, planktonic or benthic assemblages, and community distribution that changes as a function of pH and salinity may influence the δ^2H_{HBI} (Smol and Stoermer, 2010). HBIs found in samples taken at shallow lake water depths likely produced by benthic diatoms may

differ in δ^2H when compared to δ^2H_{HBI} from samples taken at deeper water depths where planktonic diatoms are producing the HBIs. Distinguishing $\varepsilon_{HBI/lw}$ differences between diatom communities will have implications for hydroclimate interpretations of δ^2H_{HBI} if a shift in diatom community is suspected. Previous work has indicated that peak production in C_{20} HBI occurs in June, suggesting there might be seasonal influences on δ^2H_{HBI} as a proxy for δ^2H_{lw} in lakes that have greater variation in δ^2H_{lw} throughout the year than the lakes in this study (Hird and Rowland, 1995). Further work confirming this seasonality by exploring $\varepsilon_{HBI/lw}$ in lakes with short residence times whose δ^2H_{lw} changes seasonally will aid in interpretations of paleoclimate records of δ^2H_{HBI}.

5. Conclusions

This pilot dataset of δ^2H_{HBI} and δ^2H_{lw} from the Adirondacks demonstrates that diatom derived HBIs are a proxy for lake water isotopes. We find that $\varepsilon_{HBI/lw}$ between δ^2H_{HBI} and δ^2H_{lw} is largely consistent in deep samples between lakes and has the potential to be applied to sediment archives to reconstruct past δ^2H_{lw}. Sediment samples acquired at shallow depth (<4 m) have a more negative fractionation which we hypothesize changes as a function of diatom growth habitat. Similar patterns with water depths are observed in $\delta^{13}C_{HBI}$ suggesting that $\delta^{13}C_{HBI}$ may be used to differentiate between growth habits. Further work to expand this dataset to other kinds of lakes in other regions will validate the utility of δ^2H_{HBI} as a proxy for δ^2H_{lw}.

Acknowledgements

We thank Helen Eifert and Elliot Boyd for field assistance. We also thank Jonathan DeSantis and Barbara Lucas-Wilson of the New York State Department of Environmental Conservation for their assistance with sampling permits, and the Adirondack Mountain Club for granting access to Heart Lake. We thank Sarah

Hammer for laboratory support. This research was supported by the US National Science Foundation grants EAR-1229114 to AFD, EAR-1636740 (to AFD and TVL), EAR-1636744 to AK Stewart and EAR-1602789 to TVL. Acknowledgment is made to the Donors of the American Chemical Society Petroleum Research Fund for partial support of the research (PRF #60163-ND2 to AFD).

Appendix A. Supplementary data:

The supplementary data and information to this article can be accessed online at (insert link to supplement here). Water isotope data is publicly available on waterisotopes.org, Project ID, #269. HBI isotope data is available on PANGAEA (https://doi.org/10.1594/PANGAEA.922297).

References:

Aichner, B., Herzschuh, U., Wilkes, H., Vieth, A., Böhner, J., 2010. δD values of *n*-alkanes in Tibetan lake sediments and aquatic macrophytes–A surface sediment study and application to a 16 ka record from Lake Koucha. Organic Geochemistry 41, 779-790.

Anderson, L., Berkelhammer, M., Barron, J.A., Steinman, B.A., Finney, B.P., Abbott, M.B., 2016. Lake oxygen isotopes as recorders of North American Rocky Mountain hydroclimate: Holocene patterns and variability at multi-decadal to millennial time scales. Global and Planetary Change 137, 131-148.

Athanasakoglou, A., Grypioti, E., Michailidou, S., Ignea, C., Makris, A.M., Kalantidis, K., Massé, G., Argiriou, A., Verret, F., Kampranis, S.C., 2019. Isoprenoid biosynthesis in the diatom Haslea ostrearia. New Phytologist 222, 230-243.

Bade, D.L., Carpenter, S.R., Cole, J.J., Hanson, P.C., Hesslein, R.H., 2004. Controls of δ^{13}C-DIC in lakes: Geochemistry, lake metabolism, and morphometry. Limnology and Oceanography 49, 1160-1172.

Balascio, N.L., D'Andrea, W.J., Gjerde, M., Bakke, J., 2018. Hydroclimate variability of High Arctic Svalbard during the Holocene inferred from hydrogen isotopes of leaf waxes. Quaternary Science Reviews 183, 177-187.

Balascio, N.L., Zhang, Z., Bradley, R.S., Perren, B., Dahl, S.O., Bakke, J., 2011. A multi-proxy approach to assessing isolation basin stratigraphy from the Lofoten Islands, Norway. Quaternary Research 75, 288-300.

Belt, S.T., Allard, W.G., Massé, G., Robert, J.-M., Rowland, S.J., 2000. Highly branched isoprenoids (HBIs): identification of the most common and abundant sedimentary isomers. Geochimica et Cosmochimica Acta 64, 3839-3851.

Belt, S.T., Brown, T.A., Smik, L., Tatarek, A., Wiktor, J., Stowasser, G., Assmy, P., Allen, C.S., Husum, K., 2017. Identification of C_{25} highly branched isoprenoid (HBI) alkenes in diatoms of the genus Rhizosolenia in polar and sub-polar marine phytoplankton. Organic geochemistry 110, 65-72.

Belt, S.T., Massé, G., Allard, W.G., Robert, J.-M., Rowland, S.J., 2001. Identification of a C_{25} highly branched isoprenoid triene in the freshwater diatom Navicula sclesvicensis. Organic Geochemistry 32, 1169-1172.

Belt, S.T., Massé, G., Rowland, S.J., Poulin, M., Michel, C., LeBlanc, B., 2007. A novel chemical fossil of palaeo sea ice: IP_{25}. Organic Geochemistry 38, 16-27.

Berke, M.A., Cartagena Sierra, A., Bush, R., Cheah, D., O'Connor, K., 2019. Controls on leaf wax fractionation and δ^2H values in tundra vascular plants from western Greenland. Geochimica et Cosmochimica Acta 244, 565-583.

Binford, M.W., 1990. Calculation and uncertainty analysis of ^{210}Pb dates for PIRLA project lake sediment cores. Journal of Paleolimnology 3, 253-267.

Binford, M.W., Kahl, J.S., Norton, S.A., 1993. Interpretation of ^{210}Pb profiles and verification of the CRS dating model in PIRLA project lake sediment cores. Journal of Paleolimnology 9, 275-296.

Birks, H.J.B., Ter Braak, C.J.F., Line, J.M., Juggins, S., Stevenson, A.C., Battarbee, R.W., Mason, B.J., Renberg, I., Talling, J.F., 1990. Diatoms and pH reconstruction. Philosophical Transactions of the Royal Society of London. B, Biological Sciences 327, 263-278.

Bowen, G.J., 2020. The Online Isotopes in Precipitation Calculator, version 3.1. Accessible at http://www.waterisotopes.org.

Bowen, G.J., Revenaugh, J., 2003. Interpolating the isotopic composition of modern meteoric precipitation. Water Resources Research 39, 1299.

Charles, D.F., 1984. Recent pH history of Big Moose Lake (Adirondack Mountains, New York, USA) inferred from sediment diatom assemblages. Internationale Vereinigung für theoretische und angewandte Limnologie: Verhandlungen 22, 559-566.

Charles, D.F., 1985. Relationships between Surface Sediment Diatom Assemblages and Lakewater Characteristics in Adirondack Lakes. Ecology 66, 994-1011.

Charles, D.F., Binford, M.W., Furlong, E.T., Hites, R.A., Mitchell, M.J., Norton, S.A., Oldfield, F., Paterson, M.J., Smol, J.P., Uutala, A.J., 1990. Paleoecological investigation of recent lake acidification in the Adirondack Mountains, NY. Journal of Paleolimnology 3, 195-241.

Chikaraishi, Y., Naraoka, H., 2003. Compound-specific δD– $\delta^{13}C$ analyses of n-alkanes extracted from terrestrial and aquatic plants. Phytochemistry 63, 361-371.

Christie, C.E., Smol, J.P., 1986. Recent and long-term acidification of Upper Wallface Pond (NY) as indicated by mallomonadacean microfossils. Hydrobiologia 143, 355-360.

Cluett, A.A., Thomas, E.K., 2020. Resolving combined influences of inflow and evaporation on western Greenland lake water isotopes to inform paleoclimate inferences. Journal of Paleolimnology, 251-268.

Corcoran, M.C., Thomas, E.K., Boutt, D.F., 2019. Event-Based Precipitation Isotopes in the Laurentian Great Lakes Region Reveal Spatiotemporal Patterns in Moisture Recycling. Journal of Geophysical Research: Atmospheres 124, 5463-5478.

Davis, R.B., 1987. Paleolimnological diatom studies of acidification of lakes by acid rain: An application of quaternary science. Quaternary Science Reviews 6, 147-163.

Diefendorf, A.F., Freeman, K.H., Wing, S.L., 2012. Distribution and carbon isotope patterns of diterpenoids and triterpenoids in modern temperate C3 trees and their geochemical significance. Geochimica et Cosmochimica Acta 85, 342-356.

Diefendorf, A.F., Patterson, W.P., Holmden, C., Mullins, H.T., 2008. Carbon isotopes of marl and lake sediment organic matter reflect terrestrial landscape change during the late Glacial and early Holocene (16,800 to 5,540 cal yr BP): a multiproxy study of lacustrine sediments at Lough Inchiquin, western Ireland. Journal of Paleolimnology 39, 101-115.

Dion-Kirschner, H., McFarlin, J.M., Masterson, A.L., Axford, Y., Osburn, M.R., 2020. Modern constraints on the sources and climate signals recorded by sedimentary plant waxes in west Greenland. Geochimica et Cosmochimica Acta.

Dixit, S.S., Cumming, B.F., Birks, H., Smol, J.P., Kingston, J.C., Uutala, A.J., Charles, D.F., Camburn, K.E., 1993. Diatom assemblages from Adirondack lakes (New York, USA) and the development of inference models for retrospective environmental assessment. Journal of Paleolimnology 8, 27-47.

Dixit, S.S., Smol, J.P., Kingston, J.C., Charles, D.F., 1992. Diatoms: powerful indicators of environmental change. Environmental Science & Technology 26, 22-33.

Driscoll, C.T., Newton, R.M., Gubala, C.P., Baker, J.P., Christensen, S.W., 1991. Adirondack mountains, Acidic deposition and aquatic ecosystems. Springer, pp. 133-202.

Feakins, S.J., Bentley, L.P., Salinas, N., Shenkin, A., Blonder, B., Goldsmith, G.R., Ponton, C., Arvin, L.J., Wu, M.S., Peters, T., West, A.J., Martin, R.E., Enquist, B.J., Asner, G.P., Malhi, Y., 2016. Plant leaf wax biomarkers capture gradients in hydrogen isotopes of precipitation from the Andes and Amazon. Geochimica et Cosmochimica Acta 182, 155-172.

Freimuth, E.J., Diefendorf, A.F., Lowell, T.V., 2017. Hydrogen isotopes of *n*-alkanes and *n*-alkanoic acids as tracers of precipitation in a temperate forest and implications for paleorecords. Geochimica et Cosmochimica Acta 206, 166-183.

Freimuth, E.J., Diefendorf, A.F., Lowell, T.V., Bates, B.R., Schartman, A., Bird, B.W., Landis, J.D., Stewart, A.K., 2020. Contrasting sensitivity of lake sediment *n*-alkanoic acids and *n*-alkanes to basin-scale vegetation and regional-scale precipitation δ^2H in the Adirondack Mountains, NY (USA). Geochimica et Cosmochimica Acta 268, 22-41.

Fritz, S.C., Juggins, S., Battarbee, R.W., Engstrom, D.R., 1991. Reconstruction of past changes in salinity and climate using a diatom-based transfer function. Nature 352, 706-708.

Gat, J.R., 1996. Oxygen and hydrogen isotopes in the hydrological cycle. Annual Review of Earth and Planetary Sciences 24, 225-262.

Gearing, P., Gearing, J.N., Lytle, T.F., Lytle, J.S., 1976. Hydrocarbons in 60 northeast Gulf of Mexico shelf sediments: a preliminary survey. Geochimica et Cosmochimica Acta 40, 1005-1017.

Graça, J., Santos, S., 2007. Suberin: A Biopolyester of Plants' Skin. Macromolecular Bioscience 7, 128-135.

He, D., Simoneit, B.R., Jara, B., Jaffé, R., 2015. Occurrence and distribution of monomethylalkanes in the freshwater wetland ecosystem of the Florida Everglades. Chemosphere 119, 258-266.

He, D., Simoneit, B.R.T., Xu, Y., Jaffé, R., 2016. Occurrence of unsaturated C_{25} highly branched isoprenoids (HBIs) in a freshwater wetland. Organic Geochemistry 93, 59-67.

Henderson, A.K., Shuman, B.N., 2009. Hydrogen and oxygen isotopic compositions of lake water in the western United States. Geological Society of America Bulletin 121, 1179-1189.

Hepp, J., Tuthorn, M., Zech, R., Mügler, I., Schlütz, F., Zech, W., Zech, M., 2015. Reconstructing lake evaporation history and the isotopic composition of precipitation by a coupled $\delta^{18}O$–$\delta^{2}H$ biomarker approach. Journal of Hydrology 529, 622-631.

Herczeg, A.L., 1987. A Stable Carbon Isotope Study of Dissolved Inorganic Carbon Cycling in a Softwater Lake. Biogeochemistry 4, 231-263.

Hird, S.J., Rowland, S.J., 1995. An investigation of the sources and seasonal variations of highly branched isoprenoid hydrocarbons in intertidal sediments of the Tamar Estuary, UK. Mar Environ Res 40, 423-437.

Hollander, D.J., McKenzie, J.A., 1991. CO_2 control on carbon-isotope fractionation during aqueous photosynthesis: A paleo-pCO_2 barometer. Geology 19, 929-932.

Holtvoeth, J., Whiteside, J.H., Engels, S., Freitas, F.S., Grice, K., Greenwood, P., Johnson, S., Kendall, I., Lengger, S.K., Lücke, A., Mayr, C., Naafs, B.D.A., Rohrssen, M., Sepúlveda, J., 2019. The paleolimnologist's guide to compound-specific stable isotope analysis – An introduction to principles and applications of CSIA for Quaternary lake sediments. Quaternary Science Reviews 207, 101-133.

IAEA/WMO, 2020. Global Network of Isotopes in Precipitation. The GNIP Database. Accessible at https://nucleus.iaea.org/wiser.

Jones, M.C., Anderson, L., Keller, K., Nash, B., Littell, V., Wooller, M., Jolley, C.A., 2019. An Assessment of Plant Species Differences on Cellulose Oxygen Isotopes From Two Kenai Peninsula, Alaska Peatlands: Implications for Hydroclimatic Reconstructions. Frontiers in Earth Science 7.

Laird, K.R., Cumming, B.F., Wunsam, S., Rusak, J.A., Oglesby, R.J., Fritz, S.C., Leavitt, P.R., 2003. Lake sediments record large-scale shifts in moisture regimes across the northern prairies of North America during the past two millennia. Proceedings of the National Academy of Sciences 100, 2483-2488.

Laird, K.R., Fritz, S.C., Cumming, B.F., Grimm, E.C., 1998. Early-Holocene limnological and climatic variability in the Northern Great Plains. The Holocene 8, 275-285.

Laird, K.R., Kingsbury, M.V., Lewis, C.M., Cumming, B.F., 2011. Diatom-inferred depth models in 8 Canadian boreal lakes: inferred changes in the benthic: planktonic depth boundary and implications for assessment of past droughts. Quaternary Science Reviews 30, 1201-1217.

Laxson, C., Yerger, E., Favreau, H., Regalado, S., Kelting, D., 2019. Adirondack Lake Assessment Program: 2018 Report. Report.

Leng, M.J., Marshall, J.D., 2004. Palaeoclimate interpretation of stable isotope data from lake sediment archives. Quaternary Science Reviews 23, 811-831.

Massé, G., Belt, S.T., Rowland, S.J., Rohmer, M., 2004. Isoprenoid biosynthesis in the diatoms Rhizosolenia setigera (Brightwell) and Haslea ostrearia (Simonsen). Proceedings of the National Academy of Sciences 101, 4413-4418.

McFarlin, J.M., Axford, Y., Masterson, A.L., Osburn, M.R., 2019. Calibration of modern sedimentary δ^2H plant wax-water relationships in Greenland lakes. Quaternary Science Reviews 225, 105978.

McKirdy, D.M., Thorpe, C.S., Haynes, D.E., Grice, K., Krull, E.S., Halverson, G.P., Webster, L.J., 2010. The biogeochemical evolution of the Coorong during the mid- to late Holocene: An elemental, isotopic and biomarker perspective. Organic Geochemistry 41, 96-110.

Miyajima, T., Yamada, Y., Wada, E., Nakajima, T., Koitabashi, T., Hanba, Y.T., Yoshii, K., 1997. Distribution of greenhouse gases, nitrite, and $\delta^{13}C$ of dissolved inorganic carbon in Lake Biwa: Implications for hypolimnetic metabolism. Biogeochemistry 36, 205-221.

Mueller, K.E., Polissar, P.J., Oleksyn, J., Freeman, K.H., 2012. Differentiating temperate tree species and their organs using lipid biomarkers in leaves, roots and soil. Organic Geochemistry 52, 130-141.

Muschitiello, F., Andersson, A., Wohlfarth, B., Smittenberg, R.H., 2015. The C_{20} highly branched isoprenoid biomarker–a new diatom-sourced proxy for summer trophic conditions? Organic Geochemistry 81, 27-33.

Nichols, P.D., Palmisano, A.C., Volkman, J.K., Smith, G.A., White, D.C., 1988. Occurence of an isoprenoid C_{25} diunasaturated alkene and high neutral lipid content in Antractic sea-ice diatom communities Journal of Phycology 24, 90-96.

NOAA, 2020. National Climatic Data Center (NCDC). Global Historical Climatology Network. Accessible at https://www.ncdc.noaa.gov.

Olson, D.M., Dinerstein, E., Wikramanayake, E.D., Burgess, N.D., Powell, G.V.N., Underwood, E.C., D'amico, J.A., Itoua, I., Strand, H.E., Morrison, J.C., Loucks, C.J., Allnutt, T.F., Ricketts, T.H., Kura, Y., Lamoreux, J.F., Wettengel, W.W., Hedao, P., Kassem, K.R., 2001. Terrestrial Ecoregions of the World: A New Map of Life on Earth: A new global map of terrestrial ecoregions provides an innovative tool for conserving biodiversity. BioScience 51, 933-938.

Patrick, R., 1977. Ecology of freshwater diatoms and diatom communities, In: Werner, D. (Ed), The biology of diatoms. University of California Press, Berkeley, CA, pp. 284-332.

Peel, M.C., Finlayson, B.L., McMahon, T.A., 2007. Updated world map of the Köppen-Geiger climate classification. Hydrology and Earth System Sciecnes Discussions 4, 439-473.

Pisani, O., Louda, J.W., Jaffé, R., 2013. Biomarker assessment of spatial and temporal changes in the composition of flocculent material (floc) in the subtropical wetland of the Florida Coastal Everglades. Environmental Chemistry 10, 424-436.

Polissar, P.J., D'Andrea, W.J., 2014. Uncertainty in paleohydrologic reconstructions from molecular δD values. Geochimica et Cosmochimica Acta 129, 146-156.

Pollard, M., Beisson, F., Li, Y., Ohlrogge, J.B., 2008. Building lipid barriers: biosynthesis of cutin and suberin. Trends in Plant Science 13, 236-246.

Rach, O., Kahmen, A., Brauer, A., Sachse, D., 2017. A dual-biomarker approach for quantification of changes in relative humidity from sedimentary lipid D/H ratios. Clim. Past 13, 741-757.

Rowland, S., Robson, J., 1990. The widespread occurrence of highly branched acyclic C_{20}, C_{25} and C_{30} hydrocarbons in recent sediments and biota—a review. Mar Environ Res 30, 191-216.

Rowland, S., Yon, D., Lewis, C., Maxwell, J., 1985. Occurrence of 2, 6, 10-trimethyl-7-(3-methylbutyl)-dodecane and related hydrocarbons in the green alga Enteromorpha prolifera and sediments. Organic Geochemistry 8, 207-213.

Rühland, K.M., Paterson, A.M., Smol, J.P., 2015. Lake diatom responses to warming: reviewing the evidence. Journal of Paleolimnology 54, 1-35.

Sachse, D., Billault, I., Bowen, G.J., Chikaraishi, Y., Dawson, T.E., Feakins, S.J., Freeman, K.H., Magill, C.R., McInerney, F.A., Van der Meer, M.T.J., Polissar, P., Robins, R.J., Sachs, J.P., Schmidt, H.-L., Sessions, A.L., White, J.W.C., West, J.B., Kahmen, A., 2012. Molecular Paleohydrology: Interpreting the Hydrogen-Isotopic Composition of Lipid Biomarkers from Photosynthesizing Organisms. Annual Review of Earth and Planetary Sciences 40, 221-249.

Sauer, P.E., Eglinton, T.I., Hayes, J.M., Schimmelmann, A., Sessions, A.L., 2001. Compound-specific D/H ratios of lipid biomarkers from sediments as a proxy for environmental and climatic conditions. Geochimica et Cosmochimica Acta 65, 213-222.

Schartman, A.K., Diefendorf, A.F., Lowell, T.V., Freimuth, E.J., Stewart, A.K., Landis, J.D., Bates, B.R., 2020. Stable source of Holocene spring precipitation recorded in leaf wax hydrogen-isotope ratios from two New York lakes. Quaternary science reviews 240, 106357.

Seckbach, J., 2019. Diatoms: fundamentals and applications. Wiley, Salem, Massachusetts;Hoboken, New Jersey.

Shero, B.R., Parker, M., Stewart, K.M., 1978. The diatoms, productivity and morphometry of 43 lakes in New York State, USA. Internationale Revue der gesamten Hydrobiologie und Hydrographie 63, 365-387.

Sinninghe Damsté, J.S., Schouten, S., Rijpstra, W.I.C., Hopmans, E.C., Peletier, H., Gieskes, W.W.C., Geenevasen, J.A.J., 1999. Structural identification of the C_{25} highly branched isoprenoid pentaene in the marine diatom Rhizosolenia setigera. Organic Geochemistry 30, 1581-1583.

Smol, J.P., Stoermer, E.F., 2010. The diatoms: applications for the environmental and earth sciences. Cambridge University Press.

Soininen, J., Teittinen, A., 2019. Fifteen important questions in the spatial ecology of diatoms. Freshwater Biology 64, 2071-2083.

Stager, J.C., Cumming, B.F., Laird, K.R., Garrigan-Piela, A., Pederson, N., Wiltse, B., Lane, C.S., Nester, J., Ruzmaikin, A., 2017. A 1600-year diatom record of hydroclimate variability from Wolf Lake, New York. The Holocene 27, 246-257.

Street-Perrott, F.A., Holmes, J.A., Robertson, I., Ficken, K.J., Koff, T., Loader, N.J., Marshall, J.D., Martma, T., 2018. The Holocene isotopic record of aquatic cellulose from Lake Äntu Sinijärv, Estonia: Influence of changing climate and organic-matter sources. Quaternary Science Reviews 193, 68-83.

Thomas, E.K., Briner, J.P., Ryan-Henry, J.J., Huang, Y., 2016. A major increase in winter snowfall during the middle Holocene on western Greenland caused by reduced sea ice in Baffin Bay and the Labrador Sea. Geophysical Research Letters 43, 5302-5308.

Thomas, E.K., Hollister, K.V., Cluett, A.A., Corcoran, M.C., 2020. Reconstructing Arctic precipitation seasonality using aquatic leaf wax δ^2H in lakes with contrasting residence times. Paleoceanography and Paleoclimatology 35, e2020PA003886.

Tipple, B.J., Pagani, M., 2013. Environmental control on eastern broadleaf forest species' leaf wax distributions and D/H ratios. Geochimica et Cosmochimica Acta 111, 64-77.

van Geldern, R., Barth, J.A.C., 2012. Optimization of instrument setup and post-run corrections for oxygen and hydrogen stable isotope measurements of water by isotope ratio infrared spectroscopy (IRIS). Limnology and oceanography, methods 10, 1024-1036.

Volkman, J.K., Barrett, S.M., Blackburn, S.I., Mansour, M.P., Sikes, E.L., Gelin, F., 1998. Microalgal biomarkers: a review of recent research developments. Organic Geochemistry 29, 1163-1179.

Wolfe, B.B., Falcone, M.D., Clogg-Wright, K.P., Mongeon, C.L., Yi, Y., Brock, B.E., Amour, N.A.S., Mark, W.A., Edwards, T.W., 2007. Progress in isotope paleohydrology using lake sediment cellulose. Journal of Paleolimnology 37, 221-231.

Zhang, Z., Sachs, J.P., 2007. Hydrogen isotope fractionation in freshwater algae: I. Variations among lipids and species. Organic Geochemistry 38, 582-608.

Figure 1

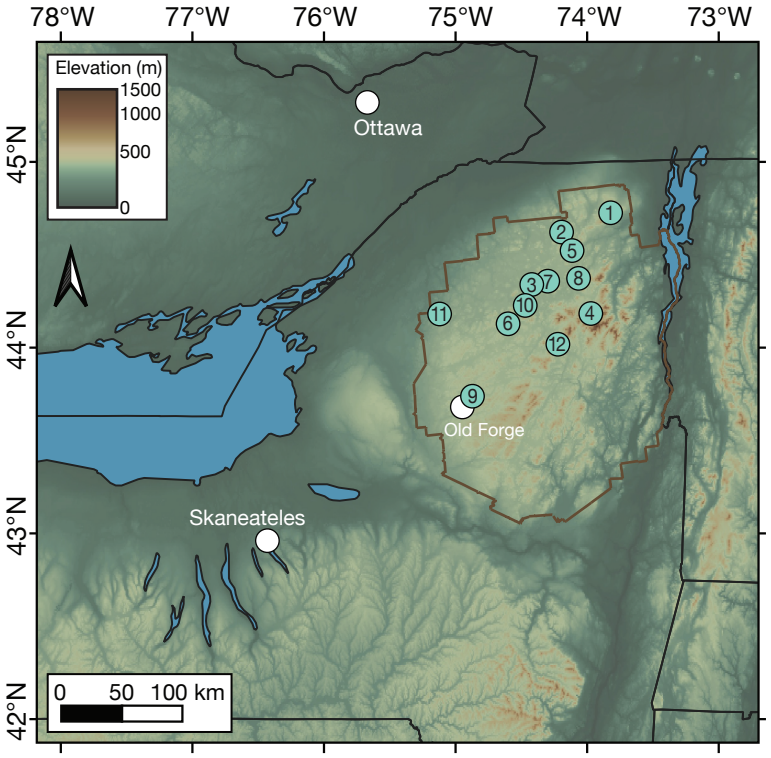
78°W
77°W
76°W
75°W
74°W
73°W
45°N
44°N
43°N
42°N
Elevation (m)
1500
1000
500
0
Ottawa
Old Forge
Skaneateles
0 50 100 km
1
2
5
3
7
8
10
11
6
4
12
9

Figure 1 caption

Figure 1: Elevation map of the 12 sampled lakes in the Adirondacks Mountains, NY: 1, Chazy Lake; 2, Debar Pond; 3, East Pine Pond; 4, Heart Lake; 5, Hope Lake; 6, Horseshoe Lake; 7, Little Green Pond; 8, Moose Pond; 9, Quiver Pond; 10, Raquette Lake; 11, Sucker Lake; 12, Wolf Lake. Brown line outlines the Adirondack State Park. White dots illustrate the locations of precipitation isotope, temperature and precipitation amount data used (Corcoran et al., 2019; IAEA/WMO, 2020; NOAA, 2020).

Figure 2

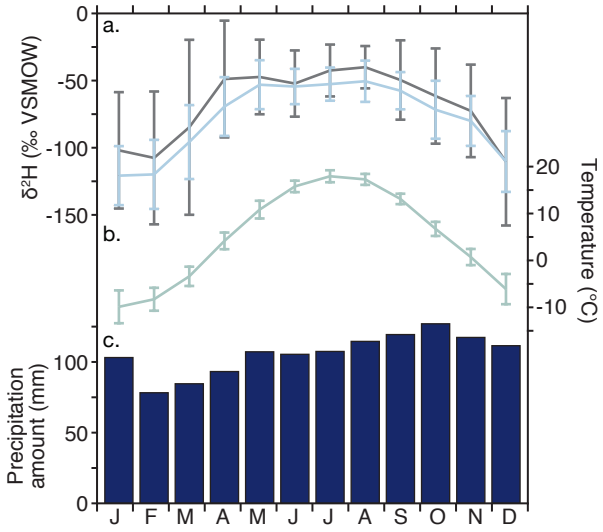
a.
b.
c.
δ²H (‰ VSMOW)
Temperature (°C)
Precipitation amount (mm)
0
-50
-100
-150
20
10
0
-10
100
50
0
J F M A M J J A S O N D

Figure 2 caption

Figure 2: Modern climate of the Adirondacks, NY. a) Average monthly precipitation δ^2H from Skaneateles (gray) and Ottawa, ON, (blue) for 2015 - 2018 and 1972 – 2017 respectively (Corcoran et al., 2019; IAEA/WMO, 2020). Error bars are the standard deviation of all samples taken during that month for all years. b) Average monthly temperature are from Old Forge, NY for 1971 – 2010 (NOAA, 2020). Error bars are the same as in b). c) Average monthly precipitation amount from Old Forge, NY for 1971 – 2010.

Figure 3

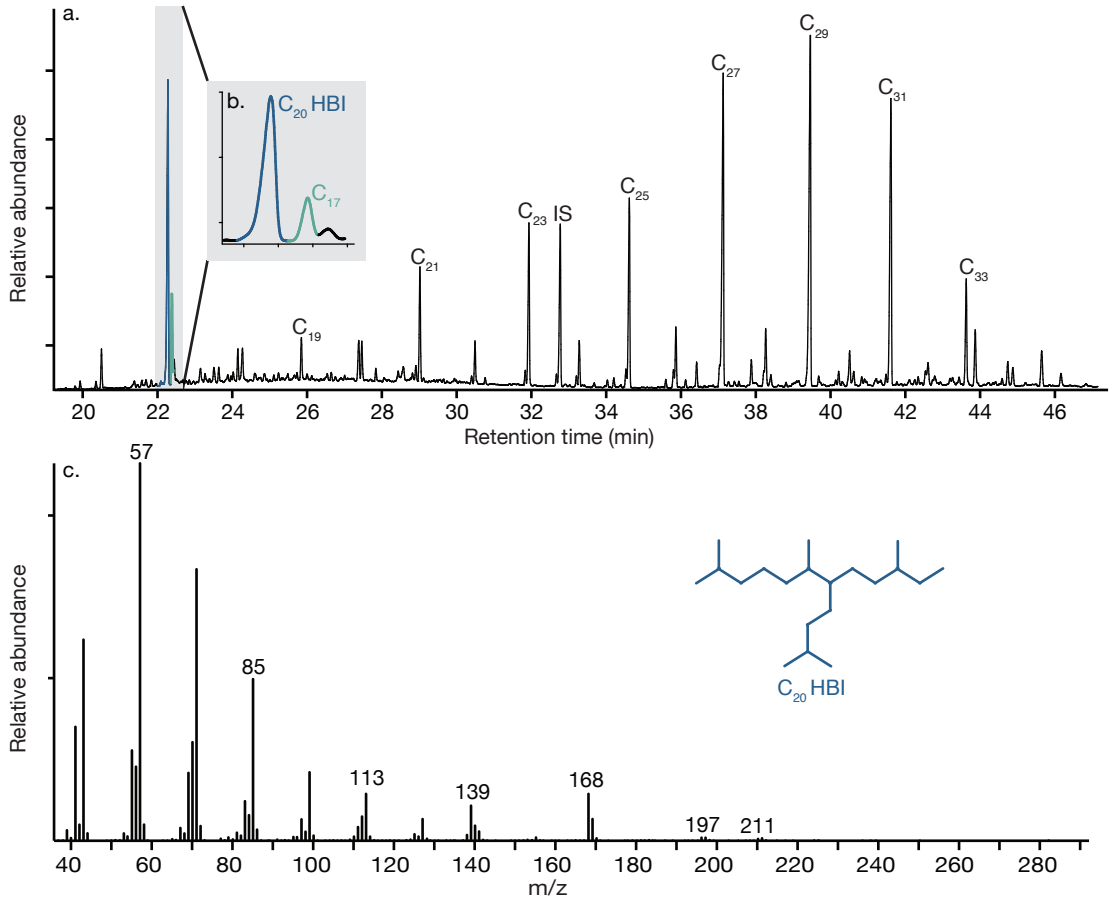
a.
b.
C20 HBI
C17
C19
C21
C23 IS
C25
C27
C29
C31
C33
Relative abundance
Retention time (min)
c.
57
85
113
139
168
197
211
m/z
C20 HBI

Figure 3 caption

Figure 3: Partial GC chromatogram of the hydrocarbon fraction from a lake surface sediment sample from Moose Pond, Adirondacks Mountains, NY. a) A partial GC-FID chromatogram of highly branched isoprenoids and alkanes extracted from the sediment. b) C_{20} HBI and C_{17} alkane highlighted to show separation of these two compounds. Prior to δ^2H analysis of the C_{20} HBI, samples were further purified using urea adduction to remove the C_{17} alkane which could not be adequately separated on the GC-IRMS. c) Mass spectrum of C_{20} HBIs.

Figure 4

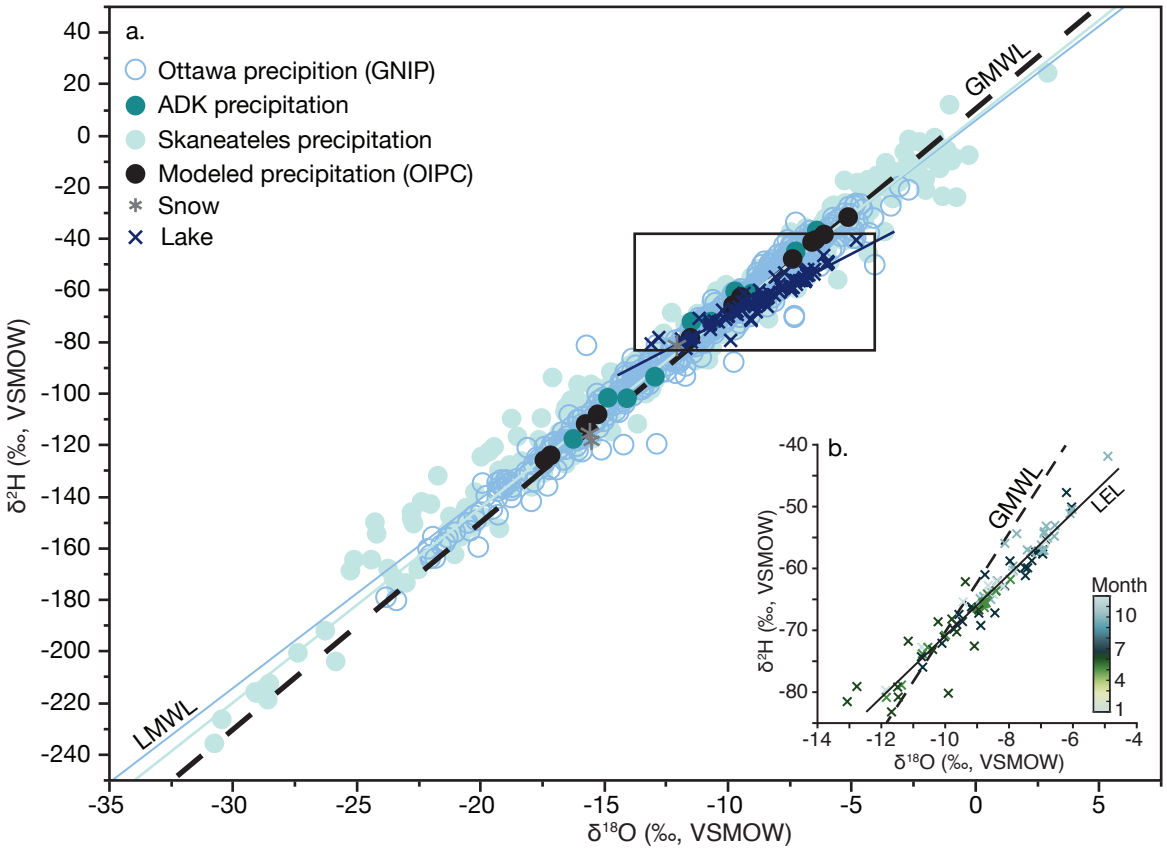
a.
Ottawa precipition (GNIP)
ADK precipitation
Skaneateles precipitation
Modeled precipitation (OIPC)
Snow
Lake
GMWL
LMWL
δ²H (‰, VSMOW)
δ¹⁸O (‰, VSMOW)
b.
GMWL
LEL
Month
10
7
4
1
δ²H (‰, VSMOW)
δ¹⁸O (‰, VSMOW)

Figure 4 caption

Figure 4: Plot of lake water and precipitation δ^2H and $\delta^{18}O$. a) Precipitation δ^2H and $\delta^{18}O$ from Skaneateles, NY, Ottawa, ON and the Adirondacks are light green, dark green and blue open circles (Corcoran et al., 2019; Freimuth et al., 2020; IAEA/WMO, 2020). Modelled OIPC precipitation are black circles (Bowen, 2020; Bowen et al., 2005; IAEA/WMO, 2020). Gray snowflakes are collected snow from lake catchments in the Adirondacks. Crosses are sampled Adirondacks lake water δ^2H and $\delta^{18}O$. Global meteoric water line (GMWL), local meteoric water line (LMWL) and local evaporative line (LEL) are plotted. b) Lake water δ^2H and $\delta^{18}O$ plotted with the local evaporation line. Colors correspond to sampling month where months 1-12 are January-December.

Figure 5

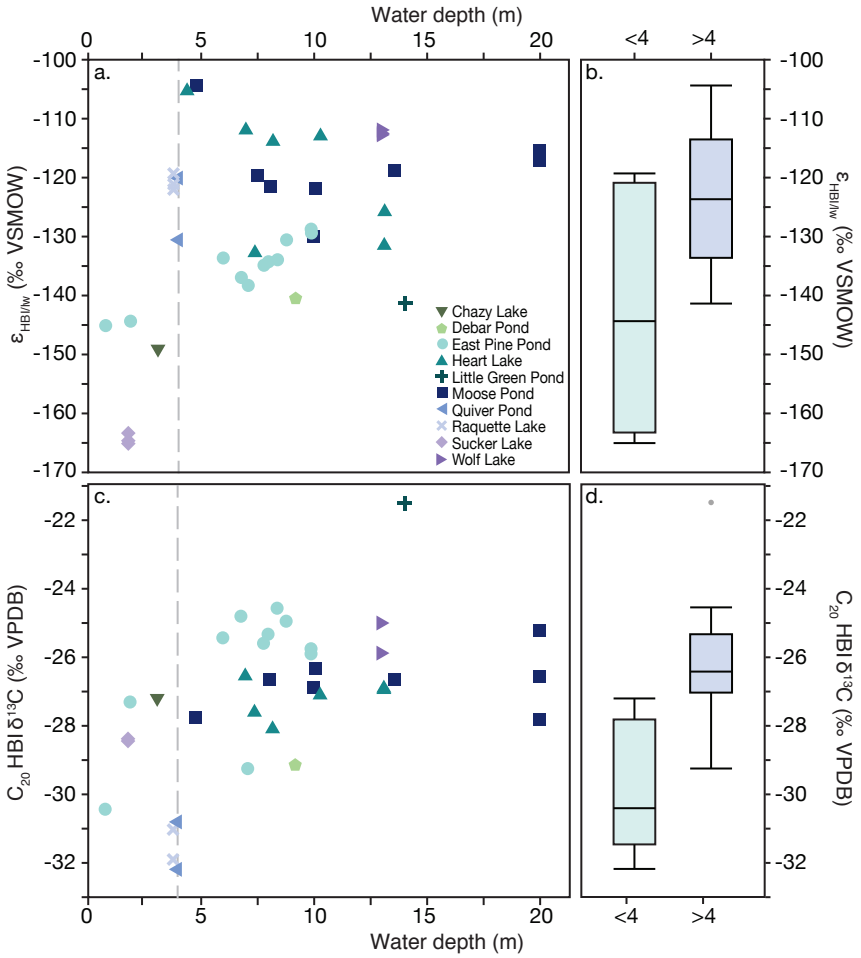
Water depth (m)
a.
b.
c.
d.
$\varepsilon_{HBI/lw}$ (‰ VSMOW)
C_{20} HBI $\delta^{13}C$ (‰ VPDB)
<4
>4
Chazy Lake
Debar Pond
East Pine Pond
Heart Lake
Little Green Pond
Moose Pond
Quiver Pond
Raquette Lake
Sucker Lake
Wolf Lake

Figure 5 caption

Figure 5: Relationship of $\varepsilon_{HBI/lw}$ and $\delta^{13}C_{HBI}$ by depth. a) Scatter plot of $\varepsilon_{HBI/lw}$ by water depth of sediment sampling locations. Colors and symbols correspond to the sampled lake. b) box and whisker plot of $\varepsilon_{HBI/lw}$ above and below 4 m of lake depth. Boxes are quartiles about the median, whiskers are 5 and 95 percentiles and gray circles are outliers, c) and d) are the same as a) and b) but for $\delta^{13}C_{HBI}$.

Table 1

Table 1: Adirondack lake properties including location, elevation, lake area, catchment area, lake conductivity and lake water δ^2H and $\delta^{18}O$

Lake Name	**Latitude**	**Longitude**	**Elevation (m)**	**Conductivity (μS)**	**Lake area (km^2)**	**Catchment area (km^2)**	**Maximum depth (m)**	**Lake water δ^2H**	**Lake water $\delta^{18}O$**
Chazy Lake	44.7258	-73.8208	466	79	7.5	58	30.0	-71.0	-10.0
Debar Pond	44.6219	-74.1936	483	29	0.4	6.4	9.1	-66.1	-9.1
East Pine Pond	44.3383	-74.4150	513	23	0.3	1.1	10.1	-62.7	-8.2
Heart Lake	44.1825	-73.9693	665	8	0	0.8	12.2	-61.7	-8.0
Hope Lake	44.5132	-74.1253	523	12	0.1	0.4	11.5	-59.3	-7.5
Horseshoe Lake	44.1356	-74.6219	524		1.6	11.5	4.9	-62.2	-8.3
Little Green Pond	44.3574	-74.2989	521	24	0.3	1.4	12.2	-60.3	-7.7
Moose Pond	44.3717	-74.0620	475	26	0.7	17.4	21.3	-72.3	-10.1
Quiver Pond	43.7379	-74.8709	539		0.1	0.6	2.0	-55.5	-6.9
Raquette Lake	44.2268	-74.4700	470		4.1	17.1	29.0	-67.8	-9.8
Sucker Lake	44.1808	-75.1208	426	34	0.4	2.6	3.0	-45.9	-5.5
Wolf Lake	44.0179	-74.2217	558		0.6	4.7	14.0	-66.5	-9.5